



# Reactivity of chloroacetamides toward sulfide + black carbon: Insights from structural analogues and dynamic NMR spectroscopy



Xiaolei Xu<sup>a</sup>, Priyansh D. Gujarati<sup>b</sup>, Neechi Okwor<sup>b</sup>, John D. Sivey<sup>b</sup>, Keith P. Reber<sup>b</sup>, Wenqing Xu<sup>a,\*</sup>

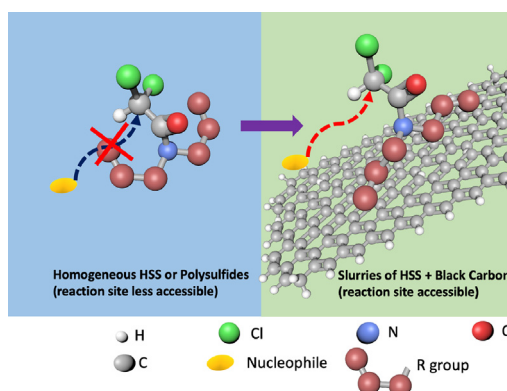
<sup>a</sup> Department of Civil and Environmental Engineering, Villanova University, Villanova, PA 19085, USA

<sup>b</sup> Department of Chemistry, Towson University, Towson, MD 21252, USA

## HIGHLIGHTS

- Assessed the impact of increasing —Cl substituents on reaction kinetics and pathways of chloroacetamides.
- Adsorption onto black carbon significantly altered chloroacetamide reactivity relative to the homogeneous system.
- Conformational changes upon adsorption may influence the reactivity of chloroacetamides.

## GRAPHICAL ABSTRACT



## ARTICLE INFO

### Article history:

Received 30 June 2021

Received in revised form 22 August 2021

Accepted 27 August 2021

Available online 3 September 2021

Editor: Yolanda Picó

### Keywords:

Halogenated agrochemical fate

Dechlorination

Polysulfides

Subsurface environments

Dynamic NMR spectroscopy

## ABSTRACT

Chloroacetamides are commonly used in herbicide formulations, and their occurrence has been reported in soils and groundwater. However, how their chemical structures affect transformation kinetics and pathways in the presence of environmental reagents such as hydrogen sulfide species and black carbon has not been investigated. In this work, we assessed the impact of increasing Cl substituents on reaction kinetics and pathways of six chloroacetamides. The contribution of individual pathways (reductive dechlorination vs. nucleophilic substitution) to the overall decay of selected chloroacetamides was differentiated using various experimental setups; both the transformation rates and product distributions were characterized. Our results suggest that the number of Cl substituents affected reaction pathways and kinetics: trichloroacetamides predominantly underwent reductive dechlorination whereas mono- and dichloroacetamides transformed via nucleophilic substitution. Furthermore, we synthesized eight dichloroacetamide analogs ( $\text{Cl}_2\text{CHC}(=\text{O})\text{NRR}'$ ) with differing R groups and characterized their transformation kinetics. Dynamic NMR spectroscopy was employed to quantify the rotational energy barriers of dichloroacetamides. Our results suggest that adsorption of dichloroacetamides on black carbon constrained R groups from approaching the dichloromethyl carbon and subsequently favored nucleophilic attack. This study provides new insights to better predict the fate of chloroacetamides in subsurface environments by linking their structural characteristics to transformation kinetics and pathways.

© 2021 Elsevier B.V. All rights reserved.

## 1. Introduction

Chloroacetamides ( $\text{Cl}_x\text{CH}_3\text{-}_x\text{C}(=\text{O})\text{NRR}'$ ,  $x = 1,2,3$ ) are widely used in herbicide formulations (Abu-Qare and Duncan, 2002; Davies and

\* Corresponding author.

E-mail address: [wenqing.xu@villanova.edu](mailto:wenqing.xu@villanova.edu) (W. Xu).

Caseley, 1999; EPA; Jablonkai, 2013). For example, the monochloroacetamide herbicide *S*-metolachlor is applied at a rate of approximately  $2.5 \times 10^6$  kg-yr<sup>-1</sup> in the U.S. and has been frequently detected in groundwater and soil (Helling et al., 1971; Hladik et al., 2008; Kolpin et al., 1998; Williams et al., 2014; Woodward et al., 2018). Dichloroacetamide safeners, such as AD-67 (AD), benoxacor (BD), and dichlormid (AID), are often paired with a monochloroacetamide or thiocarbamate herbicide to protect crops from herbicide toxicity (Abu-Qare and Duncan, 2002). The application rate of dichloroacetamide safeners in the U.S. is approximately  $2 \times 10^6$  kg-yr<sup>-1</sup> (Sivey and Roberts, 2012). Despite the influx of dichloroacetamides into the environment, information on their environmental fate is scarce relative to herbicide active ingredients, possibly due to the “inert” regulatory status of dichloroacetamide safeners (Kral et al., 2019; Ricko et al., 2020; Sivey et al., 2015; Sivey and Roberts, 2012; Su et al., 2019; Woodward et al., 2018; Xu et al., 2020). Nonetheless, residual AID has been reported in the range of 0.01–0.02 mg-kg<sup>-1</sup> in soils after 21 days of application (Wilson and James, 1987). Furthermore, AD, BD, and AID have been detected in streams in the Midwestern United States (Woodward et al., 2018). Due to their moderate-to-high mobility (Acharya et al., 2020; Acharya and Weidhaas, 2018; Davies and Caseley, 1999; Jablonkai, 2013), chloroacetamides are anticipated to enter subsurface environments where black carbon and hydrogen sulfide species (HSS) can co-exist.

Black carbon (e.g., charcoal) is a naturally-occurring geosorbent that constitutes 1–20% of the total organic carbon mass in soils and sediments (Lian and Xing, 2017; Middelburg et al., 1999). Black carbon can sequester chemicals by nonspecific (e.g., van der Waals) and specific (e.g.,  $\pi$ - $\pi$ ) interactions, serving as an important sink for organic pollutants (Keilweit et al., 2010; Lian and Xing, 2017). HSS (i.e., the sum of H<sub>2</sub>S, HS<sup>-</sup>, and S<sup>2-</sup>) often co-exist with black carbon in subsurface environments at concentrations up to the mM range (Barbash and Reinhard, 1989b; Dunnette et al., 1985; Heitmann and Blodau, 2006; King et al., 1982; Kristiana et al., 2010). Previous studies suggest that HSS can act as a nucleophile or reductant for the abiotic transformation of chloroacetamides, dihalomethanes, chloroazines, and hexachloroethane, potentially decreasing their toxicity (Barbash and Reinhard, 1989a; Lippa and Roberts, 2002; Loch et al., 2002; Miller et al., 1998). However, such reactions are often kinetically slow (Barbash and Reinhard, 1989a; Roberts et al., 1992; Wu et al., 2006). Nevertheless, recent research demonstrated that the synergy between black carbon and HSS significantly promoted the abiotic transformation rates of chloroacetamide herbicides and safeners by 4–200 fold (Xu et al., 2020). Similar observations were reported for other compounds such as nitroaromatics, chlorinated solvents, and dichlorodiphenyltrichloroethane (DDT) (Ding and Xu, 2016; Oh et al., 2013; Saquing et al., 2016; Xu et al., 2010; Xu et al., 2013; Xu et al., 2015). Two of the putative mechanisms for such enhancement include (1) accelerated electron transfer by the graphitic regions of black carbon, resulting in faster contaminant reduction (Xu et al., 2010) and (2) oxidation of HSS by black carbon to generate polysulfides that are stronger nucleophiles than HSS (Xu et al., 2020; Zhao et al., 2019). Yet, little is known regarding how contaminant chemical structures affect their transformation kinetics and reaction pathways in the presence of black carbon and HSS that are ubiquitous in subsurface environments.

The goal of this study was to evaluate the relationship between chloroacetamide structural characteristics and their transformation kinetics/pathways by black carbon and HSS using chloroacetamide analogs as model compounds. We used graphite as a model black carbon with high carbon content (~99.99 wt%) and minimal functional groups and is non-porous (Ding and Xu, 2016; Xu et al., 2013; Xu et al., 2020). First, we assessed the impact of the number of Cl substituents on reaction kinetics and pathways of six chloroacetamides. The contribution of individual pathways (i.e., reductive dechlorination vs. nucleophilic substitution; Scheme S1) to the overall chloroacetamide decay

was differentiated using four model systems (HSS systems, slurries of graphite + HSS, polysulfides systems, and electrochemical cells), where both the transformation rates and product distributions were analyzed. Furthermore, we characterized the transformation kinetics of eight dichloroacetamide analogs containing R groups that differ in size and chemical identity (e.g., alkyl, allyl, cycloalkyl, and phenyl moieties) in the presence of HSS and graphite. Dynamic (i.e., variable-temperature) proton nuclear magnetic resonance (<sup>1</sup>H NMR) spectroscopy was employed to quantify the rotational energy barriers of eight dichloroacetamide analogs in the presence of solvents with different polarities. The findings from this study enable better predictions of how chemical structure influences transformations in subsurface environments for chloroacetamides and potentially other halogenated contaminants.

## 2. Material and methods

### 2.1. Chemical reagents

All chloroacetamides used in this study were either purchased from chemical vendors or synthesized. Detailed information on the sources and purity of these chemicals is provided in Text S1. Monochloroacetamides included *N,N*-dipropyl-2-chloroacetamide (PC) and *N,N*-diallyl-2-chloroacetamide (AIC). Dichloroacetamides included three herbicide safeners (benoxacor (BD), AD-67 (AD), and dichlormid (AID)) and five structural analogs (*N,N*-dipropyl-2,2-dichloroacetamide (PD), *N,N*-diethyl-2,2-dichloroacetamide (ED), *N,N*-dipentyl-2,2-dichloroacetamide (PeD), *N,N*-dicyclohexyl-2,2-dichloroacetamide (ChD), and *N,N*-diphenyl-2,2-dichloroacetamide (PhD)). Trichloroacetamides included *N,N*-dipropyl-2,2,2-trichloroacetamide (PT) and *N,N*-diallyl-2,2,2-trichloroacetamide (AIT).

### 2.2. Reaction systems

To differentiate the operative reaction pathways, we monitored chloroacetamide decay kinetics and, for selected compounds, analyzed the associated transformation products in four experimental setups (i.e., HSS systems, slurries of graphite + HSS, polysulfides systems, and electrochemical cells) housed in 14 mL borosilicate vials. Details for each setup are provided below. We also carried out adsorption kinetics experiments to determine the adsorption rates for all dichloroacetamides (Fig. S1). The adsorption onto 21 g-L<sup>-1</sup> graphite powder reached equilibrium in 30 s for all dichloroacetamides, which is significantly shorter than their observed transformation half-lives in slurries of graphite + HSS (e.g., 6.3 h for AID – the shortest among the dichloroacetamides investigated). Therefore, adsorption is ostensibly not rate-limiting in slurries of graphite + HSS. MOPS buffer (10 mM, pH 6.9 ± 0.1) was purged with N<sub>2</sub> for 2 h and stored in a glovebox (5% H<sub>2</sub>, 20% CO<sub>2</sub>, 75% N<sub>2</sub>, O<sub>2</sub> < 5 ppm, Coy Laboratory Products). HSS stock solution (70 mM) was freshly prepared by dissolving Na<sub>2</sub>S·9H<sub>2</sub>O in the MOPS buffer. Both graphite powder and graphite sheet were examined in separate reactors. Chloroacetamide stock solutions (4 mM) were prepared in N<sub>2</sub>-purged acetonitrile and stored in gas-tight amber glass vials in the glovebox. All 14 mL borosilicate vials were vortexed for ~20 s and then placed on an end-over-end rotator (30 rpm) in the dark in an incubator (VWR International) at 25.0 ± 0.8 °C during the experimental timeframe unless otherwise specified.

#### 2.2.1. Slurries of graphite + HSS

To 14 mL borosilicate vials were added pre-weighed graphite powder or graphite sheet (21 g·L<sup>-1</sup>), HSS stock solution (1 mL), and a sufficient amount of MOPS buffer to reach ~90% of the total vial volume. Chloroacetamide stock solution (100 μL) was then spiked into the vials before the headspace was eliminated with MOPS buffer. The final concentration for HSS in the slurries of graphite + HSS was 5 mM.

Final concentrations of chloroacetamide were 20–24  $\mu\text{M}$  unless otherwise specified. Controls were set up in the absence of HSS or graphite powder.

### 2.2.2. Homogeneous HSS systems or polysulfides systems

MOPS buffer and 1 mL HSS stock solution were introduced to 14 mL borosilicate vials in the absence of graphite to achieve a final concentration of 5 mM HSS. Polysulfides ( $\text{S}_n^{2-}$ ) were prepared by dissolving 1.2 mM elemental sulfur ( $\text{S}_8$ ) into the 5 mM HSS solution and equilibrating for 4 weeks (Lippa and Roberts, 2002; Xu et al., 2020); final concentrations of HSS,  $\text{S}_8$ , and  $\text{S}_n^{2-}$  (by S atom) were determined to be 4.8 mM, 500  $\mu\text{M}$ , and 450  $\mu\text{M}$  following the protocols described in the chemical analysis section (Xu et al., 2020). These concentrations were similar to the measured concentrations of HSS (4.4 mM),  $\text{S}_8$  (500  $\mu\text{M}$ ), and  $\text{S}_n^{2-}$  (420  $\mu\text{M}$ ) in the slurries of graphite + HSS and thus allowed for comparison of reduced sulfur reactivity across different experimental setups. Chloroacetamide stock solution (100  $\mu\text{L}$ ) was spiked into 14 mL borosilicate vials to initiate the reaction.

### 2.2.3. Electrochemical cells

We followed previously established protocols in setting up electrochemical cells (Ding and Xu, 2016; Xu et al., 2015). Specifically, two pieces of 0.13-mm thick graphite sheet ( $21 \text{ g}\cdot\text{L}^{-1}$ ) were used as the cathode and anode, respectively, separated in two 14 mL borosilicate vials and attached to a copper wire with conductive NEM tape through a Teflon septum (Ding and Xu, 2016; Xu et al., 2015). The electrical circuit was completed by a salt bridge (1 M  $\text{K}_2\text{SO}_4$ ) in Teflon tubing. The anodic and cathodic cells contained 5 mM HSS and 15–20  $\mu\text{M}$  chloroacetamides, respectively. The mixing in the electrochemical cells was accomplished by a 3-mm magnetic stir bar (100 rpm).

## 2.3. Chemical analysis

At various time intervals, samples were collected for chemical analysis. Samples of the slurries of graphite + HSS were first centrifuged (Forma Scientific 5678) at 3000 rpm for 3 min. Aqueous supernatants were directly analyzed using a C18 column on a Shimadzu HPLC-PDA. Solid phases were extracted by shaking with 5.0 mL of acetonitrile for 3 min; the extracts were subsequently analyzed on HPLC. Extraction efficiencies for all chloroacetamides investigated were 84%–102%. Detailed information regarding extraction efficiency, elution time, wavelength for detection, and mobile phase composition for chloroacetamides are summarized in Table S1.

We also analyzed transformation products for trichloroacetamides PT and AIT. Briefly, chloride was analyzed using a Dionex ICS-500 ion chromatography with a Dionex IonPac AS22 column ( $4 \text{ mm} \times 250 \text{ mm}$ ). The eluent was comprised of  $\text{Na}_2\text{CO}_3$  (4.5 mM) and  $\text{NaHCO}_3$  (1.4 mM) at a flow rate of  $1.2 \text{ mL}\cdot\text{min}^{-1}$ . HSS was quantified colorimetrically (CLINE, 1969; Xu et al., 2020). Elemental sulfur was measured by HPLC-PDA with a mobile phase of 100% methanol and a monitoring wavelength of 254 nm. The elution time for elemental sulfur was 9 min. The aqueous phase was analyzed directly for elemental sulfur on HPLC. The solid phase was extracted using dichloromethane, and the extraction efficiency of elemental sulfur from graphite was determined as  $102 \pm 4\%$  in controls in the absence of chloroacetamides (McGuire and Hamers, 2000; Xu et al., 2020; Zheng et al., 2015). Polysulfides were quantified by the total S atoms in dimethyl-polysulfanes formed by methylation of  $\text{S}_n^{2-}$  with neat iodomethane using a modified gas chromatography–mass spectrometry (GC–MS) method (Ding et al., 2019; Kristiana et al., 2010; Xu et al., 2020; Zeng et al., 2012). More details of this method are provided in Text S2. Ultra-performance liquid chromatography interfaced with a high-resolution, quadrupole/time-of-flight mass spectrometer (UPLC–qTOF–MS) was used to analyze organic transformation products in aqueous phase and solid phase-extracts of selected systems. Detailed methodology is provided in Text S3 with UPLC mobile phase composition shown in Fig. S2.

## 2.4. Dynamic $^1\text{H}$ NMR

Dichloroacetamides have restricted rotation about the C–N amide bond; if the two *N*-substituents are different, then each conformer (*cis* and *trans*) is anticipated to experience different steric hindrance and  $\text{S}_{\text{N}}2$  reactivity at the dichloromethyl group (Carlson et al., 2006; Chupp et al., 1969). The exchange rate between *cis* and *trans* conformers corresponds to the rotational energy barrier ( $\Delta G^\ddagger$ ) of the C–N bond (Biechler and Taft, 1957; Carlson et al., 2006; Chupp and Olin, 1967). A higher  $\Delta G^\ddagger$  indicates a more geometrically rigid (less flexible) structure. For dichloroacetamides with identical *N*-substituents, restricted rotation may also attenuate steric hindrance at the dichloromethyl group (Santos et al., 2014). To permit  $\Delta G^\ddagger$  calculation for 5 dichloroacetamides, dynamic  $^1\text{H}$  NMR spectra were obtained on a JEOL 400 SS spectrometer at 400 MHz. Samples of each compound (10–15 mg) were dissolved in 1.0 mL of a deuterated solvent (obtained in sealed ampules from Cambridge Isotope Laboratories), immediately transferred to NMR tubes, and then sealed with Parafilm. Although DMSO- $d_6$  was used for most experiments, alternative solvents (i.e., toluene- $d_8$  and  $\text{D}_2\text{O}$ ) were also investigated for AID, noting that  $\Delta G^\ddagger$  values can vary with the solvation environment (Bichenkova et al., 2017; Gasparro and Kolodny, 1977; Pluth et al., 2008). Chemical shifts were reported in parts per million ( $\delta$ ), and all spectra were referenced using the residual monoprotic solvent peak (2.50 ppm for DMSO- $d_6$ , 2.09 ppm for the methyl signal of toluene- $d_8$ , and 4.79 ppm for  $\text{D}_2\text{O}$ ). Spectra were obtained at temperatures spanning from 293.15 to 423.15 K (20 °C to 150 °C), typically at 10 K intervals, depending on the boiling point of the solvent.

## 3. Results and discussion

### 3.1. Transformation of trichloroacetamides in slurries of graphite + HSS vs. electrochemical cells

Decay of trichloroacetamides (PT and AIT) was observed in the slurries of graphite + HSS and electrochemical cells (Fig. 1), coupled with the generation of chloride. Controls in the presence of graphite or MOPS buffer (but no added HSS) showed negligible decay of PT or AIT. Similarly, no decay of PT or AIT was observed in the presence of HSS without graphite (data not shown). As shown in Fig. 1A and B, transformation of PT generated its dichloroacetamide analog, PD, with a  $\Delta[\text{PD}]/\Delta[\text{PT}]$  ratio of approximately 1:1 for the first two sampling points in both the slurries of graphite + HSS and electrochemical cells. PT transformation also generated chloride at a molar ratio of 1:1 at early sampling points and increased to approximately 1:2 in slurries of graphite + HSS, while chloride was generated at a ratio of 1:1 throughout the experimental timeframe in the electrochemical cells. The concentration of PD increased and then decreased in slurries of graphite + HSS but continually accumulated in the electrochemical cells.

Similarly, as shown in Fig. 1C and D, AIT transformation in the slurries of graphite + HSS and electrochemical cells yielded its dichloroacetamide analog AID, with a  $\Delta[\text{AID}]/\Delta[\text{AIT}]$  ratio of approximately 0.4 for both types of systems. Like PD, the measured concentration of AID in the slurries of graphite + HSS first increased and then decreased, while AID continually accumulated in the electrochemical cells. AIT decay generated chloride at a molar ratio of 1:1 at early sampling points and increased to approximately 1:3 at the end in the slurries of graphite + HSS, while chloride was generated at a ratio of 1:1 throughout the experimental timeframe in the electrochemical cells. The overall mass balance of chlorine, defined as the sum of  $3 \times [\text{trichloroacetamide}] + 2 \times [\text{dichloroacetamide}] + [\text{Cl}^-]$ , is compared in Fig. 1. Specifically, over 85% of the chlorine was recovered at each sampling time for the transformation of PT in both electrochemical cells and the slurries of graphite + HSS (Fig. 1A&B), as well as for the decay of AIT in the slurries of graphite + HSS (Fig. 1C). The missing

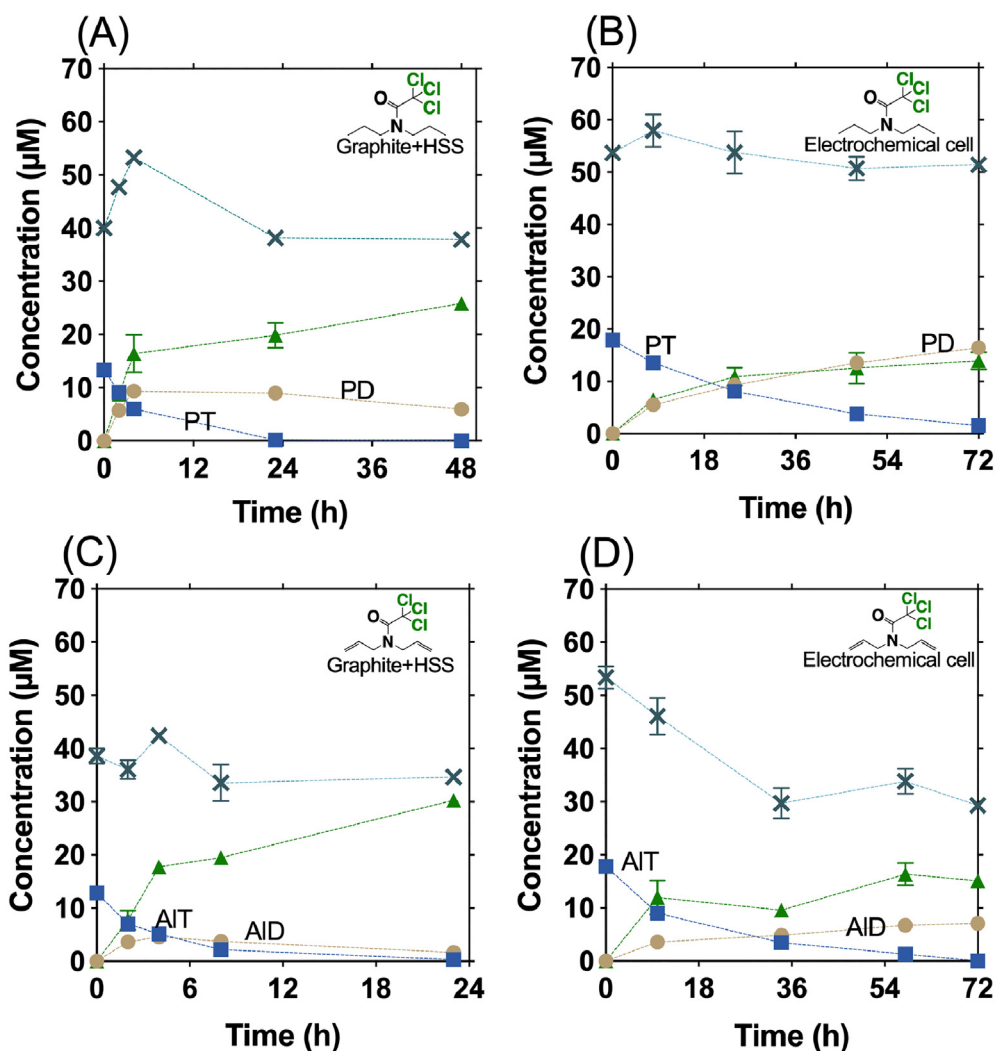


**Fig. 1.** Transformation of PT and the generation of PD in (A) slurries of graphite + HSS and (B) electrochemical cells; Transformation of AIT and the generation of AID in (C) slurries of graphite + HSS and (D) electrochemical cells. Reaction conditions:  $[HSS]_0 = 5 \text{ mM}$  in slurries of graphite + HSS or the anodic cell of electrochemical cells,  $[graphite \text{ powder}] = 21 \text{ g} \cdot \text{L}^{-1}$  in slurries of graphite + HSS,  $[graphite \text{ sheet}] = 21 \text{ g} \cdot \text{L}^{-1}$  in electrochemical cells,  $\text{pH} = 6.9 \pm 0.2$  (10 mM MOPS buffer),  $T = 25 \text{ }^\circ\text{C}$ . ■: trichloroacetamide; ●: dichloroacetamide; ▲: chloride; ×: mass balance on chlorine ( $3[\text{trichloroacetamide}] + 2[\text{dichloroacetamide}] + [\text{Cl}^-]$ ).

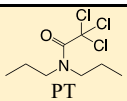
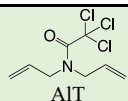
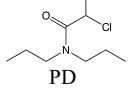
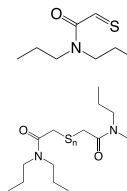
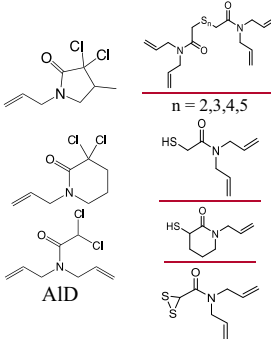
15% of the mass balance on chlorine may be a result of intermediate products that are difficult to capture. In comparison, chlorine mass balance decreased to 60% during the decay of AIT in the electrochemical cell (Fig. 1D).

Additional transformation products of PT and AIT in slurries of graphite + HSS, in polysulfides systems, and in electrochemical cells were characterized using UPLC-qTOF-MS. In the slurries of graphite + HSS, the transformation of PT and AIT generated sulfur-substituted products and their respective dichloroacetamide analogs (Table 1). PD was observed from the transformation of PT, while AID and two additional dichloroacetamide isomers were detected from the transformation of AIT. By contrast, no sulfur-substituted products were observed in the electrochemical cells for either PT or AIT; only their respective dichloroacetamide analogs were observed. In polysulfides systems, the transformation of PT and AIT generated sulfur-substituted products. Trace amount of dichloroacetamide products for both PT and AIT, namely PD, AID, and the isomers of AID were detected by the UPLC-qTOF-MS (Table 1 and S2). Quantification of these products were subsequently carried out on a HPLC-PDA as previously described in the chemical analysis section. However, their concentrations were below the MQL ( $1 \text{ } \mu\text{M}$ ). Detailed elution times and  $m/z$  data for the transformation products of PT and AIT in the slurries of graphite + HSS and in polysulfides systems are provided in Table S2.

For both PT and AIT, the generation of dichloroacetamides indicates that reductive dechlorination is an important pathway affecting the fate of these contaminants in systems containing HSS and graphite. Accumulation of dichloroacetamides in the electrochemical cells further supports the reductive dechlorination pathway (Ricko et al., 2020; Sivey and Roberts, 2012), where electron transfer from HSS (cathodic cell) to trichloroacetamide (anodic cell) ostensibly occurred. Collectively, a  $\Delta[\text{PD}]/\Delta[\text{PT}]$  ratio of approximately 1:1, a  $\Delta[\text{Cl}^-]/\Delta[\text{PT}]$  ratio of 1:1, and a chlorine mass balance of over 85% indicates that the transformation of PT proceeds via reductive dechlorination in the electrochemical cells. A lower AID yield was observed together with the generation of AID isomers in electrochemical cells, consistent with a previous study where intramolecular cyclization isomers of AID were postulated to form during reductive dechlorination of AIT with Fe(II) adsorbed on goethite or hematite (Sivey and Roberts, 2012). Due to the lack of authentic standards, we could not quantify AID isomers, which may account for the lower chlorine mass balance (~60%) for AIT (Fig. 1D).

The increase and subsequent decrease in PD and AID concentrations in slurries of graphite + HSS suggest that they are susceptible to further transformation. Completely dechlorinated sulfur-substituted products, including (multi) sulfur-bridged dimers and monomers, were observed for both PT and AIT (Table 1) in the slurries of graphite + HSS, suggesting that nucleophilic substitution occurred (Xu et al., 2020). These

**Table 1**  
Comparison of the products from trichloroacetamide transformation in electrochemical cells, polysulfides systems, and the slurries of graphite + HSS.<sup>a</sup>

Trichloroacetamide			
Products			
Slurries of Graphite + HSS	✓	✓	✓
Electrochemical cells	✓	✗	✗
Polysulfides System	✗ <sup>b</sup>	✓	✓

results are consistent with previous findings indicating that dichloroacetamides can be transformed to sulfur-substituted monomers and sulfur-bridged dimers in the slurries of graphite + HSS (Xu et al., 2020). We acknowledge that the concentrations of dichloroacetamides are likely to be lower in natural systems and the dimerization and trimerization might proceed to a lesser extent. Nonetheless, our results demonstrated that black carbon can concentrate adsorbed dichloroacetamides and subsequently favor dimerization and trimerization on black carbon surface. Overall, our results suggest that both reductive dechlorination and nucleophilic substitution are possible for the abiotic transformation of trichloroacetamides by slurries of graphite and HSS.

### 3.2. Effect of Cl substituents on abiotic transformation of chloroacetamides

To understand how the number of chlorine substituents affects transformation pathways and kinetics, we characterized the reaction rates of six mono-, di-, and trichloroacetamides (Table 2) in four experimental setups as previously described: HSS systems (no added

graphite), slurries of graphite + HSS, polysulfides systems, and electrochemical cells. The transformation of all parent compounds followed pseudo-first-order kinetics; rate constants ( $k$ ) are summarized in Table 2. In general, the addition of graphite significantly enhanced the decay rates of chloroacetamides by HSS regardless of chlorine numbers. For example, reactivity of PD was negligible in HSS systems but was greatly accelerated in slurries of graphite + HSS ( $k = 0.067 \pm 0.002 \text{ h}^{-1}$ ) with a half-life of ( $10 \pm 0.3 \text{ h}$ ).

Moreover, in slurries of graphite + HSS, the reactivity of chloroacetamides was influenced by the degree of chlorine substitution. Specifically, transformation rates of chloroacetamides in the slurries of graphite + HSS ( $k_{\text{slurries of graphite + HSS}}$ ) decreased from PT ( $0.18 \pm 0.01 \text{ h}^{-1}$ ; 3 chlorine atoms) to PD ( $0.067 \pm 0.003 \text{ h}^{-1}$ ; 2 chlorine atoms) and increased from PD to PC ( $3.5 \pm 0.2 \text{ h}^{-1}$ ; 1 chlorine atom). By contrast, in the electrochemical cells, PT showed the highest reactivity ( $k_{\text{electrochemical cells}} = 0.034 \pm 0.004 \text{ h}^{-1}$ ) while PD and PC demonstrated no appreciable reactivity. Similar trends were observed for the *N,N*-diallyl-containing compounds AIT, AID, and AIC (Table 2). In the homogeneous polysulfides systems, rate constants of chloroacetamide

**Table 2**

Effects of chlorine substituents on the observed pseudo-first-order rate constants of chloroacetamide decay in HSS systems, polysulfides systems, electrochemical cells, and slurries of graphite + HSS.<sup>a</sup>

Chloroacetamides	$k_{\text{HSS}} (\text{h}^{-1})$	$k_{\text{polysulfides}} (\text{h}^{-1})$	$k_{\text{electrochemical cell}} (\text{h}^{-1})$	$k_{\text{slurries of graphite + HSS}} (\text{h}^{-1})$
PT 	ND <sup>b</sup>	$0.013 \pm 0.004$	$0.034 \pm 0.004$ (sheet)	$0.18 \pm 0.01$ (powder) $0.043 \pm 0.003$ (sheet)
PD 	ND <sup>b</sup>	$0.034 \pm 0.003$	ND	$0.067 \pm 0.003$ (powder)
PC 	$0.50 \pm 0.02$	$2.9 \pm 0.1$	ND	$3.5 \pm 0.2$ (powder)
AIT 	ND	$0.010 \pm 0.002$	$0.046 \pm 0.003$ (sheet)	$0.21 \pm 0.01$ (powder) $0.063 \pm 0.007$ (sheet)
AID 	ND	$0.044 \pm 0.002$	ND	$0.110 \pm 0.002$ (powder)
AIC 	$0.48 \pm 0.06$	$2.7 \pm 0.4$	ND	$2.8 \pm 0.2$ (powder)

<sup>a</sup> Reaction conditions:  $[\text{HSS}]_0 = 5 \text{ mM}$  in slurries of graphite + HSS or in the anodic cell of the electrochemical cells,  $[\text{graphite powder}] = [\text{graphite sheet}] = 21 \text{ g} \cdot \text{L}^{-1}$ ,  $\text{pH} = 6.9 \pm 0.2$  (10 mM MOPS buffer), polysulfides contained 4.8 mM HSS, 500  $\mu\text{M}$  elemental sulfur, and 450  $\mu\text{M}$  polysulfides in sulfur atoms after 4-week equilibration,  $T = 25 \text{ }^\circ\text{C}$ .

<sup>b</sup> ND denotes reactivity not detectable.

transformation ( $k_{\text{polysulfides}}$ ) consistently increased as the numbers of chlorine substituents decreased from 3 to 1 for AIT ( $0.010 \pm 0.002 \text{ h}^{-1}$ ), AID ( $0.044 \pm 0.002 \text{ h}^{-1}$ ), and AIC ( $2.7 \pm 0.04 \text{ h}^{-1}$ ), or PT ( $0.013 \pm 0.004 \text{ h}^{-1}$ ), PD ( $0.034 \pm 0.003 \text{ h}^{-1}$ ), and PC ( $2.9 \pm 0.1 \text{ h}^{-1}$ ). In homogeneous HSS systems, no reactivity was observed for tri- and dichloroacetamides, whereas degradation of monochloroacetamides was observed, albeit at much slower rates compared to that observed in polysulfides systems.

The above trends can be rationalized by competing reaction pathways between reductive dechlorination and nucleophilic substitution in the slurries of graphite + HSS. Specifically, as the number of chlorine substituents increased from 1 to 3 (e.g., PC, PD, to PT), steric hindrance at the chlorine-substituted carbon increases (Anslyn and Dougherty, 2005; Bordwell and Hughes, 1983; Fernández et al., 2009), thereby attenuating nucleophilic attack at the chlorine-substituted carbon. This hypothesis is supported by observations from both HSS and polysulfides systems, where reaction rate constants decreased in the order of  $\text{PC} > \text{PD} > \text{PT}$  and  $\text{AIC} > \text{AID} > \text{AIT}$ . Our results align with previous findings that the reaction between chloroacetamide herbicides (e.g., metolachlor, acetochlor) and dichloroacetamide safeners (e.g., AID, BD) with HSS and polysulfides systems followed a nucleophilic substitution pathway in the absence of graphite (Loch et al., 2002). The observed reactivity in the electrochemical cells increased in the order of  $\text{PC} < \text{PD} < \text{PT}$  and  $\text{AIC} < \text{AID} < \text{AIT}$ , which can be explained by the increasing electrophilicity of the chlorine-substituted carbon as the number of chlorine substituents increases, thus increasing susceptibility to reductive dichlorination (Sivey and Roberts, 2012). Overall, our results suggest that the numbers of chlorine substituents on chloroacetamides can affect their transformation rates and the competition between reductive dechlorination and nucleophilic substitution pathways, with reductive dechlorination playing a predominant role in the decay of trichloroacetamide and nucleophilic substitution contributing to transformations of the di- and monochloroacetamides.

### 3.3. Effects of R group identity on transformations of dichloroacetamides in homogeneous HSS and polysulfides systems

To interrogate how R group identity affects transformation pathways and kinetics, we characterized the transformation rates of eight

dichloroacetamide structural analogs ( $\text{Cl}_2\text{CHC}(=\text{O})\text{NRR}'$ ) in homogeneous polysulfides or HSS systems. The transformation of all eight dichloroacetamide analogs followed pseudo-first-order kinetics (Fig. S3), where rate constants ( $k$ ) are summarized in Table S3. Overall, dichloroacetamides showed reactivity toward both polysulfides and HSS (Fig. 2A). Specifically, the decay rates of dichloroacetamides by polysulfides ( $k_{\text{polysulfide}}$ ) decreased following the order:  $\text{BD} (0.104 \pm 0.004 \text{ h}^{-1}) \approx \text{AD} (0.100 \pm 0.004 \text{ h}^{-1}) > \text{ChD} (0.059 \pm 0.002 \text{ h}^{-1}) > \text{ED} (0.052 \pm 0.001 \text{ h}^{-1}) > \text{AID} (0.044 \pm 0.002 \text{ h}^{-1}) > \text{PD} (0.034 \pm 0.003 \text{ h}^{-1}) > \text{PeD} (0.030 \pm 0.001 \text{ h}^{-1}) \approx \text{PhD} (0.026 \pm 0.003 \text{ h}^{-1})$ . Although the transformation rates by HSS were slower, a similar reactivity trend among dichloroacetamides was observed (Table S3).

We also measured the rotational energy barrier ( $\Delta G^\ddagger$ ) for the amide C—N bond in several dichloroacetamides using variable temperature  $^1\text{H}$  NMR. The values of  $\Delta G^\ddagger$  are shown in Fig. 2A. For ED, PD, PeD, AID, and ChD,  $\Delta G^\ddagger$  values were calculated based on the temperature-induced coalescence dynamics of the  $^1\text{H}$  NMR signal of the analogous protons on each R group (Gasparro and Kolodny, 1977; Macomber et al., 1998). When rotation is restricted for the amide bond, the analogous protons on each R group result in distinct  $^1\text{H}$  NMR chemical shifts. Taking AID as an example, the four methylene protons adjacent to N ( $\delta_{\text{A}} = 3.97$  and  $\delta_{\text{B}} = 3.85$ ) were used as the analogous protons. These peaks broadened with increasing temperature and subsequently merged at  $100^\circ\text{C}$  (Fig. 2B). This temperature was defined as the coalescence temperature and was used to calculate  $\Delta G^\ddagger$  values as described in Text S4. We employed an identical approach to calculate  $\Delta G^\ddagger$  values for ED, PD, PeD, and ChD and their  $^1\text{H}$  NMR spectra are summarized in Fig. S5-S13.

Structural complexities of AD, BD, and PhD precluded precise calculation of their  $\Delta G^\ddagger$  values; nevertheless, these  $\Delta G^\ddagger$  values could still be estimated as described in Text S4. Our results suggest that  $\Delta G^\ddagger$  values of AD and BD were higher than ChD, while the  $\Delta G^\ddagger$  of PhD was similar to PeD. Thus, we grouped the eight dichloroacetamides into two categories based on their  $\Delta G^\ddagger$  values: high  $\Delta G^\ddagger$  values (AD, BD, and ChD with  $\Delta G^\ddagger \geq 18.6 \text{ kcal}\cdot\text{mol}^{-1}$ ) vs. low  $\Delta G^\ddagger$  values (ED, PD, PeD, AID, and PhD with  $\Delta G^\ddagger \leq 16.3 \text{ kcal}\cdot\text{mol}^{-1}$ ). The highest  $\Delta G^\ddagger$  values for AD and BD are likely due to the hindered rotation of the bulky bicyclic moieties and/or steric repulsion involving the dichloroacetyl group (Bisz et al., 2018; Krishnan et al., 2017). The lower  $\Delta G^\ddagger$  values for ED, PD, PeD, and

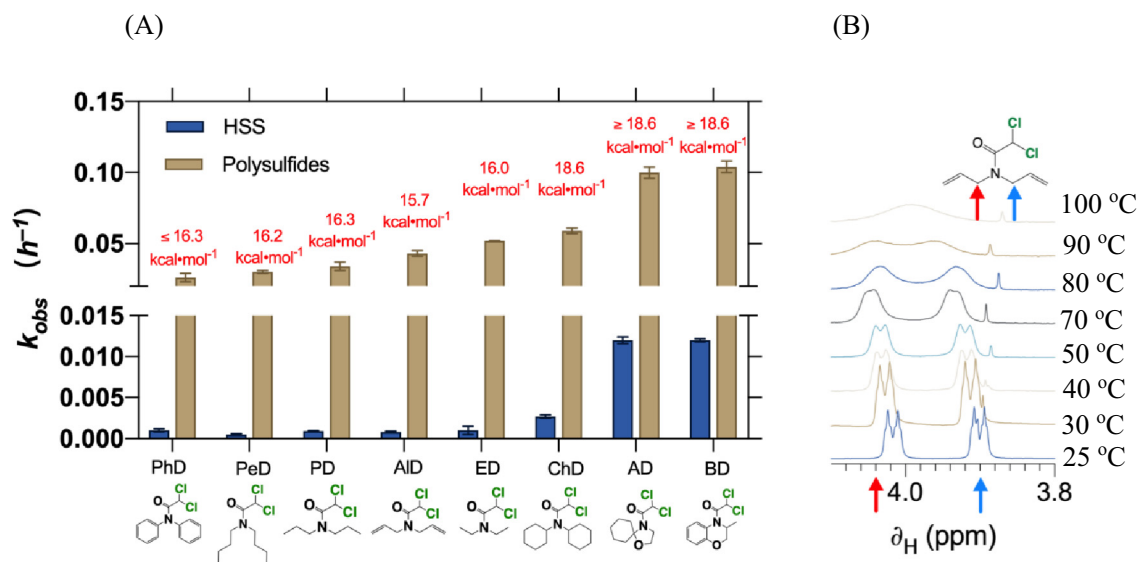


**Fig. 2.** (A) Effect of the R-group identity on the transformation kinetics of dichloroacetamides in HSS and polysulfides systems.  $\Delta G^\ddagger$  values in  $\text{kcal}\cdot\text{mol}^{-1}$  are shown on the top of each bar in red. Reaction conditions for (A): [dichloroacetamide] = 20–24  $\mu\text{M}$ , [HSS]<sub>0</sub> = 5 mM, pH =  $6.9 \pm 0.2$  (10 mM MOPS buffer), polysulfides contained 4.8 mM HSS, 500  $\mu\text{M}$  elemental sulfur, and 450  $\mu\text{M}$  polysulfides in sulfur atoms after 4-week equilibration, and T = 25 °C. (B)  $^1\text{H}$  NMR signals for the methylene protons adjacent to nitrogen, demonstrating coalescence at elevated temperature. NMR conditions: 400 MHz variable temperature  $^1\text{H}$  NMR spectra of AID in DMSO- $d_6$  at temperatures ranging from 25 to 100 °C. (For interpretation of the references to colour in this figure legend, the reader is referred to the web version of this article.)

AID can be explained by the relatively lower steric repulsion between *n*-alkyl or allyl groups and the amide bond, as well as more favorable solvation compared to cyclic structures (Pluth et al., 2008). The lower  $\Delta G^\ddagger$  value of PhD can be rationalized via an electronic effect in which the amide resonance is less effective due to a competing resonance interaction with the aromatic rings (Bisz et al., 2018; Pros and Bloomfield, 2019).

Previous studies suggested that reduced sulfur species (e.g., HSS and polysulfides systems) can react with mono- and dichloroacetamides via a bimolecular nucleophilic substitution ( $S_N2$ ) pathway (Loch et al., 2002; Xu et al., 2020). The observed differences in dichloroacetamide reactivity toward HSS or polysulfides can thus be rationalized by their R group identity. We hypothesize that the lower reactivity of ED, PD, PeD, AID, and PhD (Fig. 2A) can be explained by their relatively low  $\Delta G^\ddagger$  values, associated with less geometrically rigid R groups that enable them to adopt conformations in closer proximity to the dichloromethyl carbon (Chupp and Olin, 1967) and thus disfavoring nucleophilic attack by an  $S_N2$  pathway. The reactivity trend of ED > PD > PeD likely results from increasing steric hindrance with increasing alkyl chain length.

PhD is less reactive than ChD toward HSS and polysulfides systems, which may be attributed to the  $\pi$  electrons in phenyl groups of PhD that could disfavor the approach of an anionic nucleophile (e.g.,  $HS^-$ ) and the subsequent accumulation of negative charge in the  $S_N2$  activated complex. A previous study found that PhD was more reactive than ChD in reactions with  $Cr(H_2O)_6^{2+}$ , in which case the phenyl groups of PhD could ostensibly promote interactions between  $Cr(H_2O)_6^{2+}$  and dichloroacetamides, thereby enhancing rates of dichloroacetamide reduction (Sivey and Roberts, 2012). By contrast, despite possessing larger R groups, ChD was more reactive than PeD, which may be attributed to its geometrically rigid cyclohexyl groups (Santos et al., 2014). The higher reactivity of ChD, AD, and BD might result from their higher  $\Delta G^\ddagger$  values (Fig. 2A), consistent with more geometrically rigid R groups that were restricted from approaching the dichloromethyl carbon and thus favoring nucleophilic attack by an  $S_N2$  pathway.

### 3.4. Effect of R group identity on transformation of dichloroacetamides in the slurries of graphite + HSS

The presence of graphite significantly enhanced the reactivity of dichloroacetamides and altered the relative reactivity of dichloroacetamides toward HSS. Decay rates of dichloroacetamides in slurries of graphite + HSS ( $k_{slurries\ of\ graphite + HSS}$ , Fig. 3A) decreased in the order: AID ( $0.110 \pm 0.002\ h^{-1}$ ) > BD ( $0.083 \pm 0.003\ h^{-1}$ ) > PhD ( $0.075 \pm 0.003\ h^{-1}$ )  $\approx$  AD ( $0.075 \pm 0.003\ h^{-1}$ ) > ED ( $0.068 \pm 0.007\ h^{-1}$ )  $\geq$  PD ( $0.067 \pm 0.003\ h^{-1}$ )  $\geq$  ChD ( $0.065 \pm 0.007\ h^{-1}$ ) > PeD

( $0.060 \pm 0.002\ h^{-1}$ ). To quantify the effect of graphite on accelerating dichloroacetamide transformation rates, we defined the enhancement factor as the ratio of the rate constant from the slurries of graphite + HSS ( $k_{slurries\ of\ graphite + HSS}$ ) over those from the homogeneous HSS systems ( $k_{HSS}$ ). The trend in enhancement factors is shown in Fig. 3A, where AID ( $134 \pm 15$ )  $\approx$  PeD ( $136 \pm 30$ ) > PhD ( $98 \pm 7$ ) > PD ( $72 \pm 5$ ) > ED ( $60 \pm 7$ ) > ChD ( $24 \pm 3$ ) > BD ( $7.0 \pm 0.3$ ) > AD ( $6.3 \pm 0.3$ ).

The observed enhancement in dichloroacetamide reactivity can be explained by conformational changes upon adsorption onto graphite. Low enhancement factors were observed for BD, AD, and ChD ( $6.3$  to  $24$ ), which can be attributed to their geometrically rigid R groups (higher  $\Delta G^\ddagger$  values) that constrained conformational changes upon adsorption. By contrast, high enhancement factors ( $60$  to  $134$ ) were observed for ED, PD, PeD, AID, and PhD, which can be rationalized by their less geometrically rigid R groups (low  $\Delta G^\ddagger$  from  $15.7$  to  $16.3\ kcal\cdot mol^{-1}$ ) when dissolved in solution. As a result, the interaction between dichloroacetamides and graphite likely constrained their R groups from approaching the dichloromethyl carbon and subsequently favored nucleophilic attack via an  $S_N2$  pathway.

The observed enhancement factors increased from ED < PD < PeD. We postulate that the longer alkyl chains (ED < PD < PeD) increased the adsorption affinities due to non-specific (e.g., van der Waals) interactions between dichloroacetamides and graphite. This is further supported by the increasing fraction of ED < PD < PeD on graphite surface (Fig. S1) and the positive correlation between the HPLC retention times of ED, PD, and PeD and their enhancement factors (Fig. S4A). However, no correlation was observed when all eight dichloroacetamides were compared together (Fig. S4B), suggesting that other factors, such as specific (e.g.,  $\pi$ - $\pi$ ) interactions, should also be considered. Notably, enhancement factors were significantly higher for AID ( $134 \pm 15$ ) vs. PD ( $72 \pm 5$ ) and for PhD ( $98 \pm 7$ ) vs. ChD ( $24 \pm 3$ ). Similarly, as shown in Table 2, a higher reactivity was observed for AIT compared to PT in slurries of graphite + HSS and in electrochemical cells. These observations can be rationalized by the stronger interaction between the graphitic region of the graphite and the allyl groups of AID or AIT, or the phenyl groups of PhD. We propose that specific (e.g.,  $\pi$ - $\pi$ ) interactions between allyl or phenyl groups and the graphitic region of graphite (Zhu and Pignatello, 2005) further restricted the R groups of AID, AIT, and PhD from approaching the dichloromethyl carbon in comparison to PD, PT, and ChD, respectively, and thus favored nucleophilic attack by an  $S_N2$  pathway.

The impact of adsorption on the conformational changes of dichloroacetamides was further investigated by variable temperature

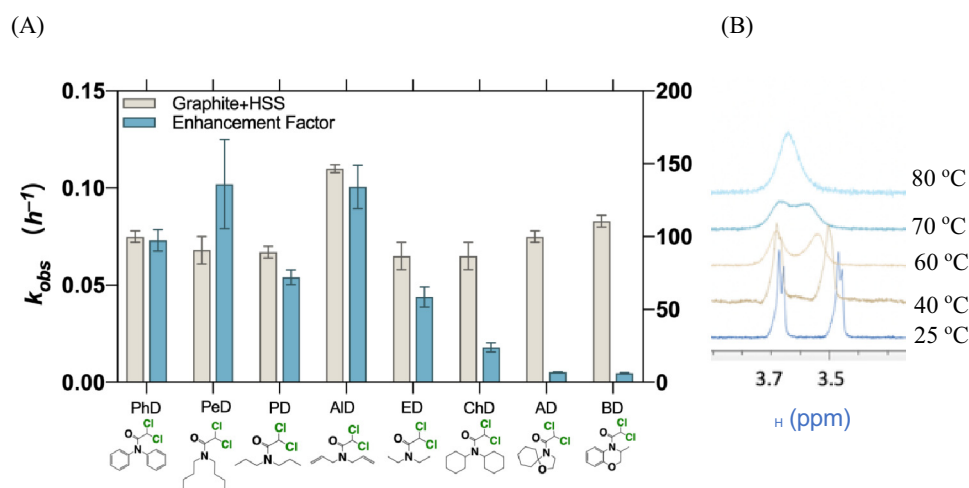


**Fig. 3.** (A) Effect of the R-group identity on the transformation kinetics of dichloroacetamides in the slurries of graphite + HSS. (B) Variable temperature  $^1H$  NMR spectra of AID in toluene- $d_8$ . Reaction conditions for (A): [dichloroacetamide] = 20–24  $\mu M$ , [HSS] $_0$  = 5 mM, pH =  $6.9 \pm 0.2$  (10 mM MOPS buffer); [graphite powder] = 21  $g\cdot L^{-1}$ , and  $T = 25\ ^\circ C$ . NMR conditions for (B): 400 MHz variable temperature  $^1H$  NMR spectra of AID in toluene- $d_8$  at temperatures ranging from 25 to 80  $^\circ C$ .

$^1\text{H}$  NMR in the presence of solvents with different polarities, including  $\text{D}_2\text{O}$ ,  $\text{DMSO-}d_6$ , and  $\text{toluene-}d_8$ . AID was selected as a model compound for investigations of such solvent effects. Fig. 3B demonstrates the  $^1\text{H}$  NMR coalescence dynamics of the analogous methylene protons of AID in  $\text{toluene-}d_8$ . The coalescence temperatures of AID decreased from 100 °C to 80 °C when dissolved in  $\text{DMSO-}d_6$  and  $\text{toluene-}d_8$ , respectively, corresponding to a decrease of  $\Delta G^\ddagger$  from 15.7 kcal·mol $^{-1}$  in  $\text{DMSO-}d_6$  to 14.9 kcal·mol $^{-1}$  in  $\text{toluene-}d_8$ . Peak coalescence was not observed for AID in  $\text{D}_2\text{O}$  as the temperatures approached the boiling point of  $\text{D}_2\text{O}$  (Fig. S13), thus preventing us from calculating a precise value of  $\Delta G^\ddagger$ .

Similar to previous studies (Cox and Lectka, 1998; Moriarty, 1963; Pluth et al., 2008), we postulate that the decrease in  $\Delta G^\ddagger$  of AID when switching from  $\text{DMSO}$  to  $\text{toluene}$  was due to differential solvation in a less polar solvent and/or  $\pi$ - $\pi$  interactions between the amide/allyl groups and  $\text{toluene}$ . The results of the variable temperature NMR experiments in  $\text{toluene-}d_8$  could be particularly relevant to the reaction of AID in slurries of black carbon + HSS. In changing from the polar, aprotic solvent  $\text{DMSO}$  to the less polar solvent  $\text{toluene}$ , the energy barrier for rotation about the amide C—N bond decreased by 0.8 kcal·mol $^{-1}$ . As a  $\pi$ -rich aromatic solvent,  $\text{toluene}$  should more closely approximate the chemical properties of graphite (Zhu et al., 2004). Therefore, it is possible that similar  $\pi$ -donor interactions between AID and the graphite surface may help to explain why AID exhibited the highest enhancement factor among the eight dichloroacetamides investigated.

#### 4. Conclusion

Our study demonstrated that the number of chlorine substituents could shift the predominant reaction pathway from nucleophilic to reductive dechlorination, which may result in products with different toxicity and biodegradability (Heckel et al., 2018; Palau et al., 2017; Palau et al., 2014). Further studies on the effect of halogen substituents in reaction pathways and their ecotoxicity profile are merited given the ubiquitous presence of halogenated organic contaminants in the environment. Additionally, this study pioneered the use of dynamic  $^1\text{H}$  NMR spectroscopy to quantify the geometrical rigidity of environmentally-relevant dichloroacetamides, elucidating the potential impact of conformational changes during the adsorption processes on the reactivity of these compounds. The application of dynamic NMR can conceivably be extended beyond dichloroacetamides as the reactivity and transformation pathways of other contaminants can also possess constrained conformations. For example, the *cis* conformers of amides are more reactive toward hydrolysis (Biechler and Taft, 1957; Carlson et al., 2006). Moreover, dehydrohalogenation of alkyl halide conformers can generate haloalkenes isomers with different reactivities toward subsequent reductive dichlorination (Seeman, 1983).

Furthermore, our finding that adsorption of dichloroacetamides on graphite significantly altered their relative reactivity (e.g., up to an enhancement factor of 134-fold) has important environmental implications. Compared to graphite, a model black carbon with minimum functional groups, naturally occurring black carbon maybe more reactive in facilitating dichloroacetamide transformation due to their abundant functional groups. Moreover, adsorption is a ubiquitous environmental process that controls the fate and transport of many pollutants. Further studies are needed to evaluate whether enhanced reactivities of contaminants occur in mineral systems upon adsorption and possibly explore the synergies between the black carbon and mineral systems (Kappler et al., 2014; Lian and Xing, 2017; Ricko et al., 2020). These endeavors could help uncover a largely overlooked pool in the environment for sequestering and transforming contaminants. Additionally, chloroacetamides are widely used as herbicide constituents (Abu-Qare and Duncan, 2002), preservatives (Perrenoud et al., 1994), pharmaceutical precursors (Fitzpatrick et al., 2018), and active pharmaceutical ingredients (Brock, 1961). Recent studies also indicate the formation of chloroacetamides as disinfection byproducts during the

chloramination of acetaldehyde and dissolved organic matter (Kimura et al., 2013; Kimura et al., 2015; Le Roux et al., 2016; Plewa et al., 2008). Thus, the findings from this study could inform industries beyond the agricultural sector and communities that are impacted by the application (or formation) of chloroacetamides. Lastly, the diverse roles of sulfur species elucidated by this study and their interaction with black carbon and contaminants could inform other areas of study, including systems where  $\text{H}_2\text{S}/\text{HS}^-$  serve as biological signaling compounds, or sensor developments using sulfur-based ligands (Pluth and Tonzetich, 2020).

#### CRedit authorship contribution statement

**Xiaolei Xu:** Data curation, Formal analysis, Methodology, Writing – original draft. **Priyansh D. Gujarati:** Formal analysis. **Neechi Okwor:** Formal analysis. **John D. Sivey:** Formal analysis, Writing – review & editing. **Keith P. Reber:** Formal analysis, Supervision, Writing – review & editing. **Wenqing Xu:** Project administration, Formal analysis, Supervision, Writing – review & editing.

#### Declaration of competing interest

The authors declare that they have no known competing financial interests or personal relationships that could have appeared to influence the work reported in this paper.

#### Acknowledgements

X.X. and W.X. thank the U.S. National Science Foundation (NSF) CAREER award (CBET-1752220) for the financial support. Funding to Towson University from NSF (CBET-1702610, CBET-1703796, CHE-0923051, and CHE-1531562) and from The Camille and Henry Dreyfus Foundation (TH-20-021) is also acknowledged.

#### Appendix A. Supplementary data

Supplementary data to this article can be found online at <https://doi.org/10.1016/j.scitotenv.2021.150064>.

#### References

- Abu-Qare, A.W., Duncan, H.J., 2002. Herbicide safeners: uses, limitations, metabolism, and mechanisms of action. *Chemosphere* 48, 965–974.
- Acharya, S.P., Weidhaas, J., 2018. Solubility, partitioning, oxidation and photodegradation of dichloroacetamide herbicide safeners, benoxacor and furilazole. *Chemosphere* 211, 1018–1024.
- Acharya, S.P., Johnson, J., Weidhaas, J., 2020. Adsorption kinetics of the herbicide safeners, benoxacor and furilazole, to activated carbon and agricultural soils. *J. Environ. Sci.* 89, 23–34.
- Anslyn, E.V., Dougherty, D.A., 2005. *Modern Physical Organic Chemistry*. University Science: Sausalito, California.
- Barbash, J.E., Reinhard, M., 1989a. Abiotic dehalogenation of 1,2-dichloroethane and 1,2-dibromoethane in aqueous solution containing hydrogen sulfide. *Environ. Sci. Technol.* 23, 1349–1358.
- Barbash, J.E., Reinhard, M., 1989b. Reactivity of Sulfur Nucleophiles Toward Halogenated Organic Compounds in Natural Waters. *Biogenic Sulfur in the Environment*. 393. American Chemical Society, pp. 101–138.
- Bichenkova, E.V., Raju, A.P.A., Burusco, K.K., Kinloch, I.A., Novoselov, K.S., Clarke, D.J., 2017. NMR detects molecular interactions of graphene with aromatic and aliphatic hydrocarbons in water. *2D Mater.* 5, 015003.
- Biechler, S.S., Taft, R.W., 1957. The effect of structure on kinetics and mechanism of the alkaline hydrolysis of Anilides. *J. Am. Chem. Soc.* 79, 4927–4935.
- Bisz, E., Piontek, A., Dziuk, B., Szostak, R., Szostak, M., 2018. Barriers to rotation in ortho-substituted tertiary aromatic amides: effect of chloro-substitution on resonance and distortion. *J. Org. Chem.* 83, 3159–3163.
- Bordwell, F.G., Hughes, D.L., 1983. Steric and electronic effects in  $\text{S}_{\text{N}}2$  reactions of 9-substituted fluorenyl and  $\alpha$ -cyano carbanions with benzyl chloride in dimethyl sulfoxide solution. *J. Org. Chem.* 48, 2206–2215.
- Brock, T.D., 1961. Chloramphenicol. *Bacteriol. Rev.* 25, 32–48.
- Carlson, D.L., Than, K.D., Roberts, A.L., 2006. Acid- and base-catalyzed hydrolysis of chloroacetamide herbicides. *J. Agric. Food Chem.* 54, 4740–4750.
- Chupp, J.P., Olin, J.F., 1967. Chemical and physical properties of some rotational isomers of  $\alpha$ -haloacetanilides. a novel unreactive halogen system. *J. Org. Chem.* 32, 2297–2303.

- Chupp, J.P., Olin, J.F., Landwehr, H.K., 1969. Structural factors influencing rotational isomerism and alkylation properties in some  $\alpha$ -haloacetanilides. *J. Org. Chem.* 34, 1192–1197.
- Cline, J.D., 1969. Spectrophotometric Determination of Hydrogen Sulfide In Natural Water. 14, pp. 454–458.
- Cox, C., Lectka, T., 1998. Solvent effects on the barrier to rotation in carbamates. *J. Org. Chem.* 63, 2426–2427.
- Davies, J., Casey, J.C., 1999. Herbicide Safeners: A Review. 55, pp. 1043–1058.
- Ding, K., Xu, W., 2016. Black carbon facilitated dechlorination of DDT and its metabolites by sulfide. *Environ. Sci. Technol.* 50, 12976–12983.
- Ding, K., Duran, M., Xu, W., 2019. The synergistic interaction between sulfate-reducing bacteria and pyrogenic carbonaceous matter in DDT decay. *Chemosphere* 233, 252–260.
- Dunnette, D.A., Chynoweth, D.P., Mancy, K.H., 1985. The source of hydrogen sulfide in anoxic sediment. *Water Res.* 19, 875–884.
- EPA US, 2020. Pesticides Industry Sales and Usage 2008 - 2012 Market Estimates.
- Fernández, I., Frenking, G., Uggerud, E., 2009. The interplay between steric and electronic effects in SN2 reactions. *Chem. Eur. J.* 15, 2166–2175.
- Fitzpatrick, D.E., Maujean, T., Evans, A.C., Ley, S.V., 2018. Across-the-world automated optimization and continuous-flow synthesis of pharmaceutical agents operating through a cloud-based server. *Angew. Chem. Int. Ed.* 57, 15128–15132.
- Gasparro, F.P., Kolodny, N.H., 1977. NMR determination of the rotational barrier in N, N-dimethylacetamide. a physical chemistry experiment. *J. Chem. Educ.* 54, 258.
- Heckel, B., McNeill, K., Elsner, M., 2018. Chlorinated ethene reactivity with vitamin B12 is governed by cobalamin chloroethylcarbanions as crossroads of competing pathways. *ACS Catal.* 8, 3054–3066.
- Heitmann, T., Blodau, C., 2006. Oxidation and incorporation of hydrogen sulfide by dissolved organic matter. *Chem. Geol.* 235, 12–20.
- Helling, C.S., Kearney, P.C., Alexander, M., 1971. Behavior of pesticides in soils. In: Brady, N.C. (Ed.), *Advances in Agronomy*. 23. Academic Press, pp. 147–240.
- Hladik, M.L., Bouwer, E.J., Roberts, A.L., 2008. Neutral degradates of chloroacetamide herbicides: occurrence in drinking water and removal during conventional water treatment. *Water Res.* 42, 4905–4914.
- Jablonkai, I., 2013. Herbicide safeners: effective tools to improve herbicide selectivity. In: APJ, Kelton (Ed.), *Herbicides—Current Research and Case Studies in Use*, Rijeka.
- Kappler, A., Wuestner, M.L., Ruecker, A., Harter, J., Halama, M., Behrens, S., 2014. Biochar as an electron shuttle between bacteria and Fe(III) minerals. *Environ. Sci. Technol. Lett.* 1, 339–344.
- Keiluweit, M., Nico, P.S., Johnson, M.G., Kleber, M., 2010. Dynamic molecular structure of plant biomass-derived black carbon (Biochar). *Environ. Sci. Technol.* 44, 1247–1253.
- Kimura, S.Y., Komaki, Y., Plewa, M.J., Mariñas, B.J., 2013. Chloroacetoneitrile and N,2-dichloroacetamide formation from the reaction of chloroacetaldehyde and monochloramine in water. *Environ. Sci. Technol.* 47, 12382–12390.
- Kimura, S.Y., Vu, T.N., Komaki, Y., Plewa, M.J., Mariñas, B.J., 2015. Acetonitrile and N-chloroacetamide formation from the reaction of acetaldehyde and monochloramine. *Environ. Sci. Technol.* 49, 9954–9963.
- King, G.M., Klug, M.J., Wiegert, R.G., Chalmers, A.G., 1982. Relation of Soil Water Movement and Sulfide Concentration to Spartina alterniflora Production in a Georgia Salt Marsh. 218, pp. 61–63.
- Kolpin, D.W., Barbash, J.E., Gilliom, R.J., 1998. Occurrence of pesticides in shallow groundwater of the United States: initial results from the National Water-Quality Assessment Program. *Environ. Sci. Technol.* 32, 558–566.
- Kral, A.E., Pflug, N.C., McFadden, M.E., LeFevre, G.H., Sivey, J.D., Cwiertyny, D.M., 2019. Photochemical transformations of dichloroacetamide safeners. *Environ. Sci. Technol.* 53, 6738–6746.
- Krishnan, V.V., Vazquez, S., Maitra, K., Maitra, S., 2017. Restricted amide rotation with steric hindrance induced multiple conformations. *Chem. Phys. Lett.* 689, 148–151.
- Kristiana, I., Heitz, A., Joll, C., Sathasivan, A., 2010. Analysis of polysulfides in drinking water distribution systems using headspace solid-phase microextraction and gas chromatography-mass spectrometry. *J. Chromatogr. A* 1217, 5995–6001.
- Le Roux, J., Nihemaiti, M., Croué, J.-P., 2016. The role of aromatic precursors in the formation of haloacetamides by chloramination of dissolved organic matter. *Water Res.* 88, 371–379.
- Lian, F., Xing, B., 2017. Black carbon (Biochar) in water/soil environments: molecular structure, sorption, stability, and potential risk. *Environ. Sci. Technol.* 51, 13517–13532.
- Lippa, K.A., Roberts, A.L., 2002. Nucleophilic aromatic substitution reactions of chloroazines with bisulfide (HS-) and polysulfides (Sn2-). *Environ. Sci. Technol.* 36, 2008–2018.
- Loch, A.R., Lippa, K.A., Carlson, D.L., Chin, Y.P., Traina, S.J., Roberts, A.L., 2002. Nucleophilic aliphatic substitution reactions of propachlor, alachlor, and metolachlor with bisulfide (HS-) and polysulfides (Sn2-). *Environ. Sci. Technol.* 36, 4065–4073.
- Macomber, R.S., Wiley, J., Sons, 1998. *A Complete Introduction to Modern NMR Spectroscopy*. Wiley.
- McGuire, M.M., Hamers, R.J., 2000. Extraction and quantitative analysis of elemental sulfur from sulfide mineral surfaces by high-performance liquid chromatography. *Environ. Sci. Technol.* 34, 4651–4655.
- Middelburg, J.J., Nieuwenhuize, J., van Breugel, P., 1999. Black carbon in marine sediments. *Mar. Chem.* 65, 245–252.
- Miller, P.L., Vasudevan, D., Gschwend, P.M., Roberts, A.L., 1998. Transformation of hexachloroethane in a sulfidic natural water. *Environ. Sci. Technol.* 32, 1269–1275.
- Moriarty, R.M., 1963. The effect of solvent upon the n.m.r. spectra of N-methylamides. I. Solvent-solute complex formation between amides and aromatic solvents. *J. Org. Chem.* 28, 1296–1299.
- Oh, S.-Y., Son, J.-G., Hur, S.H., Chung, J.S., Chiu, P.C., 2013. Black Carbon-Mediated Reduction of 2,4-Dinitrotoluene by Dithiothreitol. 42, pp. 815–821.
- Palau, J., Shouakar-Stash, O., Hunkeler, D., 2014. Carbon and chlorine isotope analysis to identify abiotic degradation pathways of 1,1,1-trichloroethane. *Environ. Sci. Technol.* 48, 14400–14408.
- Palau, J., Shouakar-Stash, O., Hattijah Mortan, S., Yu, R., Rosell, M., Marco-Urrea, E., et al., 2017. Hydrogen isotope fractionation during the biodegradation of 1,2-dichloroethane: potential for pathway identification using a multi-element (C, Cl, and H) isotope approach. *Environ. Sci. Technol.* 51, 10526–10535.
- Perrenoud, D., Bircher, A., Hunziker, T., Sutter, H., Bruckner-Tuderman, L., Stäger, J., et al., 1994. Frequency of sensitization to 13 common preservatives in Switzerland \*. *Contact Dermatitis* 30, 276–279.
- Plewa, M.J., Muellner, M.G., Richardson, S.D., Fasano, F., Buettner, K.M., Woo, Y.-T., et al., 2008. Occurrence, synthesis, and mammalian cell cytotoxicity and genotoxicity of haloacetamides: an emerging class of nitrogenous drinking water disinfection byproducts. *Environ. Sci. Technol.* 42, 955–961.
- Pluth, M.D., Tonzetich, Z.J., 2020. Hydrosulfide complexes of the transition elements: diverse roles in bioinorganic, cluster, coordination, and organometallic chemistry. *Chem. Soc. Rev.* 49, 4070–4134.
- Pluth, M.D., Bergman, R.G., Raymond, K.N., 2008. Acceleration of amide bond rotation by encapsulation in the hydrophobic interior of a water-soluble supramolecular assembly. *J. Org. Chem.* 73, 7132–7136.
- Pros, G.J., Bloomfield, A.J., 2019. Why do N-alkylated anilides bend over? The factors dictating the divergent conformational preferences of 2° and 3° N-aryl amides. *J. Phys. Chem. A* 123, 7609–7618.
- Ricko, A.N., Psoras, A.W., Sivey, J.D., 2020. Reductive transformations of dichloroacetamide safeners: effects of agrochemical co-formulants and iron oxide + manganese oxide binary-mineral systems. *Environ. Sci. Process Impacts* 22, 2104–2116.
- Roberts, A.L., Sanborn, P.N., Gschwend, P.M., 1992. Nucleophilic substitution reactions of dihalomethanes with hydrogen sulfide species. *Environ. Sci. Technol.* 26, 2263–2274.
- Santos, M.F., Braga, C.B., Rozada, T.C., Basso, E.A., Fiorin, B.C., 2014. Rotational isomerism of some chloroacetamides: theoretical and experimental studies through calculations, infrared and NMR. *Spectrochim. Acta A Mol. Biomol. Spectrosc.* 129, 148–156.
- Saquin, J.M., Yu, Y.-H., Chiu, P.C., 2016. Wood-derived black carbon (Biochar) as a microbial electron donor and acceptor. *Environ. Sci. Technol. Lett.* 3, 62–66.
- Seeman, J.L., 1983. Effect of conformational change on reactivity in organic chemistry. evaluations, applications, and extensions of Curtin-hammett winstein-holness kinetics. *Chem. Rev.* 83, 83–134.
- Sivey, J.D., Roberts, A.L., 2012. Abiotic reduction reactions of dichloroacetamide safeners: transformations of "Inert" agrochemical constituents. *Environ. Sci. Technol.* 46, 2187–2195.
- Sivey, J.D., Lehmler, H.-J., Salice, C.J., Ricko, A.N., Cwiertyny, D.M., 2015. Environmental fate and effects of dichloroacetamide herbicide safeners: "Inert" yet biologically active agrochemical ingredients. *Environ. Sci. Technol. Lett.* 2, 260–269.
- Su, L., Caywood, L.M., Sivey, J.D., Dai, N., 2019. Sunlight photolysis of safener benoxacor and herbicide metolachlor as mixtures on simulated soil surfaces. *Environ. Sci. Technol.* 53, 6784–6793.
- Williams, D.B.G., George, M.J., Marjanovic, L., 2014. Rapid detection of atrazine and metolachlor in farm soils: gas chromatography-mass spectrometry-based analysis using the bubble-in-drop single drop microextraction enrichment method. *J. Agric. Food Chem.* 62, 7676–7681.
- Wilson, R.G., James, E.R., 1987. Degradation of dichlorimid and dietholate in soils with prior EPTC, butylate, dichlorimid, and dietholate exposure. *Weed Sci.* 35, 289–294.
- Woodward, E.E., Hladik, M.L., Kolpin, D.W., 2018. Occurrence of dichloroacetamide herbicide safeners and co-applied herbicides in midwestern U.S. Streams. *Environ. Sci. Technol. Lett.* 5, 3–8.
- Wu, T., Gan, Q., Jans, U., 2006. Nucleophilic substitution of phosphorothionate Ester pesticides with bisulfide (HS-) and polysulfides (Sn2-). *Environ. Sci. Technol.* 40, 5428–5434.
- Xu, W., Dana, K.E., Mitch, W.A., 2010. Black carbon-mediated destruction of nitroglycerin and RDX by hydrogen sulfide. *Environ. Sci. Technol.* 44, 6409–6415.
- Xu, W., Pignatello, J.J., Mitch, W.A., 2013. Role of black carbon electrical conductivity in mediating Hexahydro-1,3,5-trinitro-1,3,5-triazine (RDX) transformation on carbon surfaces by sulfides. *Environ. Sci. Technol.* 47, 7129–7136.
- Xu, W., Pignatello, J.J., Mitch, W.A., 2015. Reduction of nitroaromatics sorbed to black carbon by direct reaction with sorbed sulfides. *Environ. Sci. Technol.* 49, 3419–3426.
- Xu, X., Sivey, J.D., Xu, W., 2020. Black carbon-enhanced transformation of dichloroacetamide safeners: role of reduced sulfur species. *Sci. Total Environ.* 738, 139908.
- Zeng, T., Chin, Y.-P., Arnold, W.A., 2012. Potential for abiotic reduction of pesticides in prairie pothole porewaters. *Environ. Sci. Technol.* 46, 3177–3187.
- Zhao, H.-Q., Huang, S.-Q., Xu, W.-Q., Wang, Y.-R., Wang, Y.-X., He, C.-S., et al., 2019. Undiscovered mechanism for pyrogenic carbonaceous matter-mediated abiotic transformation of azo dyes by sulfide. *Environ. Sci. Technol.* 53, 4397–4405.
- Zheng, D., Zhang, X., Li, C., ME, McKinnon, Sadok, R.G., Qu, D., 2015. Quantitative Chromatographic Determination of Dissolved Elemental Sulfur in the Non-Aqueous Electrolyte for Lithium-Sulfur Batteries. 162.
- Zhu, D., Pignatello, J.J., 2005. Characterization of aromatic compound sorptive interactions with black carbon (Charcoal) assisted by graphite as a model. *Environ. Sci. Technol.* 39, 2033–2041.
- Zhu, D., Hyun, S., Pignatello, J.J., Lee, L.S., 2004. Evidence for p-p electron donor-acceptor interactions between p-donor aromatic compounds and p-acceptor sites in soil organic matter through pH effects on sorption. *Environ. Sci. Technol.* 38, 4361–4368.